Proceedings of the 7th International Symposium on Cavitation
CAV2009 – Paper No. 109
August 16-20, 2009, Ann Arbor, Michigan, USA

Microbubble disruption by ultrasound and induced cavitation phenomena

Yukio Tomita
Hokkaido University of Education
Hakodate, Hokkaido, Japan

Ryosuke Uchikoshi
Hokkaido University of Education
Hakodate, Hokkaido, Japan

Takuya Inaba
Hokkaido University of Education
Hakodate, Hokkaido, Japan

Tetsuya Kodama
Tohoku University
Sendai, Miyagi, Japan

ABSTRACT

Aiming at the enhancement of *in vitro* sonoporation effect to cells in drug delivery, cavitation phenomena ultrasonically generated in a cylindrical vessel, which is one of a 24 well-plate, were observed with long-term photography by using a digital video camera synchronized with a repeatable flash light with the duration of 1 μs as well as by taking a number of snapshots. A suspension consisting of distilled water and microbubbles (Sonazoid ultrasound contrast agent containing C_4F_{10} gas) was used as a test liquid in the present experiment. It was found that microbubbles were rapidly destroyed after the ultrasound irradiation and their survival numbers were reduced by half at the exposure time of 100 ms. A maximum number of cavitation bubbles, sometimes more than sixty cavitation bubbles detected in the observation volume, were generated at a certain exposure time less than one second. Cavitation bubbles were mainly observed near the second products consisting of the fragments of the shell material and the flowing gas out of the interior of individual microbubbles. By exploring the free surface oscillation of a Sonazoid suspension, we found out that the (1,1) mode with the frequency of about 5 Hz was prominent. This seems important because the flow induced by this surface oscillation as well as by the acoustic radiation pressure can provide a higher possibility to convey the second products everywhere in the liquid. Consequently cavitation bubbles can be generated at a relatively long time after the ultrasound irradiation even though the majority of microbubbles are destroyed during an earlier period. In fact plenty of cavitation bubbles were occasionally generated even at the ultrasound exposure time of five seconds.

INTRODUCTION

DDS (Drug Delivery System) by using ultrasound waves in combination with microbubbles has been greatly attracted in the field of medicine and molecular biology [1, 2, 3]. If ultrasound waves interact with microbubbles encapsulating drug at an area of concern, they can be destroyed especially when the frequency of the ultrasound is very close to the resonant frequency of each microbubble. They could oscillate violently, resulting in the shell fragmentation and gas flowing out of the bubble interior. Both the gas and fragments of the destroyed material can behave as a source of cavitation nuclei. A microbubble collapsing near a cell has an ability of producing impulsive pressures [4, 5] which play as a micro-syringe to thread the cell membrane, resulting in delivering external molecular into the cell interior. This process is called sonoporation [6]. It is well recognized that the impulse due to high pressures resulting from either the micro-jet impact or the shock wave impact during the bubble collapse [7, 8] may be an important factor to temporarily permeabilize the cell membrane [9,10,11]. There are several achievements supporting this scenario. For instance, Koshiyama et al. [12] numerically confirmed the delivery of water molecule due to shock wave impulse by applying a molecular dynamics method. On the other hand Prentice et al. [13] observed a very thin liquid jet forming within a bubble in an oscillatory pressure field. From the application stand of view, it is necessary to increase the efficiency in drug delivery into cells. One of important points is to enhance sonoporation efficiency, i.e. to increase the possibility of the interaction of cavitation bubbles with cells.

In this study, therefore, the microbubble disruption and the induced cavitation bubble behavior were investigated to gain better knowledge associated with the enhancement in the number of cavitation bubbles and cell interaction. Microbubbles used in the present experiment were Sonazoid which has been commonly used as an ultrasound contrast agent (UCA) for the diagnostic around the liver. A 10% Sonazoid suspension diluted with distilled water was employed as a test liquid, together with examining tap water and distilled water. Some results regarding microbubble disruption and induced cavitation phenomena will be reported.

EXPERIMENTAL METHODS

Figure 1 shows a schematic view of the observation section. A cylindrical vessel made of polystyrene, having an

inner diameter of 16.0mm and its height of 17.9mm, was cut off from a 24well-plate, which is conventionally used in *in vitro* experiments, and set above the vibrating surface. A test liquid was a microbubble suspension with a temperature of 25ºC. Experiments using tap water and distilled water were also carried out for getting some of fundamental information associated with cavitation events. Each liquid was poured into the vessel to the level of H_L. The distance from the vibrating surface to the bottom of the vessel, H_a, was kept as 1.5mm (equivalent to one wave length λ). The bottom thickness H_b was 1.2mm. To eliminate the optical distortion through the cylindrical vessel due to light refraction, the vessel was inserted into a rectangular tank in which distilled water at the temperature of 25ºC was provided to the level of 15mm (=10λ). An encapsulated microbubble used in this experiment was a Sonazoid ultrasound contrast agent (UCA) with the shell thickness of 4nm [14] whose average diameter was about 3μm. A Sonazoid UCA contains C_4F_{10} gas inside it and is in commonly use for observing the circulation of the blood around the liver. A suspension of 16μL Sonazoid UCA and 2mL injection was defined as here an original solution and diluted with a distilled water to produce a Sonazoid suspension with the volumetric concentration of 10% v/v.

Cavitation phenomena were ultrasonically generated by making use of an ultrasound probe (Fuji Ceramic Co. HPP1038 -SUS) which has the outer diameter of 41mm and can emit ultrasound waves with the frequency f of 1MHz. If we take a burst signal to produce pressure waves, the ultrasound energy density E (J/m^2) can be expressed in the following form with the sound intensity of I (W/cm^2), the duty ratio of x (%) and the exposure time of t_{ex} (s):

$$E = 100\, x\, I\, t_{ex} \ . \qquad \text{----------} \quad (1)$$

The sound intensity I taken in the present experiment was mainly 1W/cm^2, but another value of 0.24W/cm^2 was tested in Figure 9 only for comparison. The duty ratio of 50% with the repetition number N_p of 500 and 2000 pulses were taken,

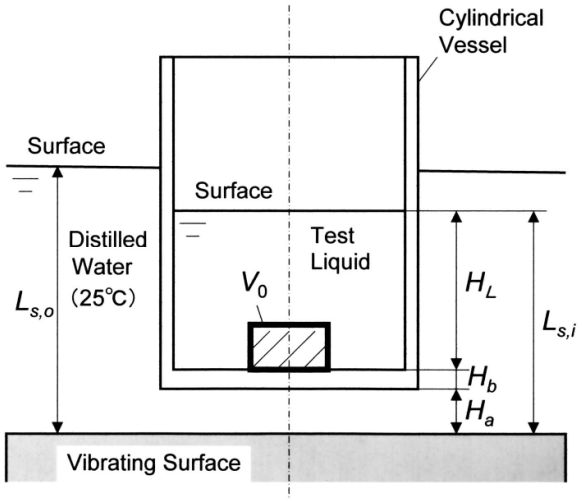

Figure 1: Schematic view of the observation section; cells are usually attached to the bottom of a cylindrical vessel

together with continuous waves (CW), i.e. the duty ratio of 100%. To generate ultrasound waves, each signal was amplified with a pulse generator (NF CDB-WF1946A) and fed to the ultrasound probe through an amplifier (NF CDB-HAS 4101). The pressure measurement in liquid was preliminarily performed by employing a hydrophone (ONDA Model HNP-1000). A wave length of an ultrasound wave in water, λ (= c/f), was calculated as 1.5mm since the sound velocity c in water was 1,497m/s at the temperature of 25ºC. In general the intensity of the permeability of a plane sound wave, propagating through two different media and going into the third medium that is the same to the first one, can be expressed as follows[15]:

$$\tau = 1/\{1+0.25\,(Z_2/Z_1-Z_1/Z_2)^2 \sin^2(2\pi H_b/\lambda_2)\}, \quad \text{-----} \quad (2)$$

where Z_i (= $\rho_i c_i$) is the acoustic impedance of the medium i (corresponding to water for i=1 and to polystyrene for i=2), ρ the density and c the sound velocity. Equation (2) suggests that an incident wave can penetrate through the vessel material without any absorption provided that the bottom thickness of the vessel satisfies the relation of $H_b/\lambda_2 = m/2$ (m=1,2,--). It was confirmed that an incident wave propagated through the polystyrene with the thickness of H_b, which corresponded to around a half of the wave length since the wave length in polystyrene, λ_2, was calculated to be 2.35mm by using the sound velocity of polystyrene, c_2 = 2,350 m/s, its density ρ_2 = 1,056 kg/m^3 and the frequency of the ultrasound wave f = 1MHz. The observation domain was limited to a volume V_0 (=2.3mm×1.6mm×3.8mm=14.0mm^3) as indicated in Figure 1, which covers the central part of the vessel including a liquid layer near the vessel bottom to which cells are normally attached. In the present experiment using a diffused light for snapshots, the distinguishable size of a bubble was 10μm. By changing the liquid depth, the repetition number and the exposure time, the microbubble disruption was examined. As a result, the microbubble survival number was counted by means of a microscope with the measuring area of 48.4μm×36.3μm with the depth of 180μm. Phenomena induced after the ultrasound irradiation were visualized with the high speed photography using a digital video camera (SONY TRV900) with the rate of 30 frames/sec which was synchronized with a repeatable flash light with its central wave length of 660nm (infrared light) and the duration t_d of 1μs (SANPICO Flash Star SP-3). Digital video images of the liquid surface fluctuation were analyzed in order to obtain the power spectra by making use of the FFT analysis. The results allowed us to provide several modes of the free surface oscillation due to the acoustic streaming induced by the pressure gradient in a liquid. In addition snapshots were taken by using a micro-flash with the duration t_d of 2μs (Sugawara MF-80) as a light source for recording an optical image on a CCD camera (Nikon Coolpix 995) which was equipped with a telesco-micro lens (Nikon ED6×18D). During this procedure a shutter was open (BULB) in a dark room.

RESULTS AND DISCUSSION

Non-linear cavitation bubble oscillation and the maximum bubble radius

It seems very difficult to measure the number of cavitation bubbles generated in an oscillatory pressure field with highly spatial and temporal resolutions because minute bubbles appear randomly and oscillate with their own short periods, growing and collapsing. Therefore, it may be meaningful to investigate the feature of a range of the maximum bubble radii to be attained for various pressure amplitudes in advance. Using the Keller-Miksis model [16], expressed in Appendix, the motion of a free bubble was numerically calculated by means of a Runge-Kutta method with the fourth degree of accuracy for various initial bubble radii and pressure amplitudes. Figure 2 shows one example of the radius versus time curve for the initial radius of R_0=3μm and the pressure amplitude of $p_A = 3p_\infty$, where p_∞ is the atmospheric pressure, f the frequency(=1MHz), ρ the water density (=997kg/m^3), μ the viscosity (=0.00089 Pa・s), σ the surface tension (=0.072N/m) and c the sound velocity in water (=1,498m/s). As clearly seen a bubble oscillates irregularly. So, it may be true that it is very difficult to measure the bubble size correctly at any instant since its motion varies too fast to observe. However, we can notice that the growth period is quite longer than the collapse period on the whole. This suggests that the possibility of capturing cavitation bubbles may be enhanced if we take snapshots for many times. The maximum bubble radius is found to be roughly three times the initial bubble radius. Calculations were carried out for the pressure amplitudes up to p_A = 1MPa although the measured pressure amplitudes were only several times the atmospheric pressure at most. The results are indicated in Figure 3. It is readily seen that the maximum bubble radius R_{max} is 17.2μm when the initial bubble radius R_0 is 1μm and for $R_0 \geq 3$μm we have $R_{max}/R_0 < 5$.

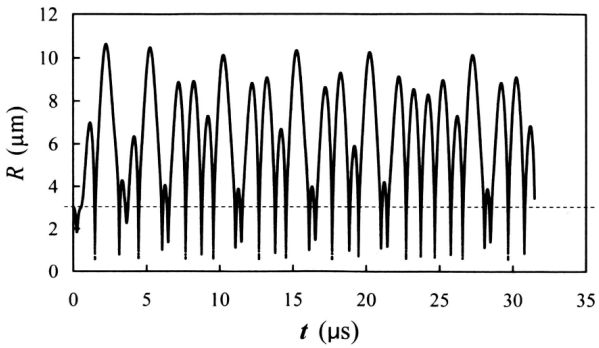

Figure 2: Non-linear bubble oscillation (R_0=3μm, p_A/p_∞= 3)

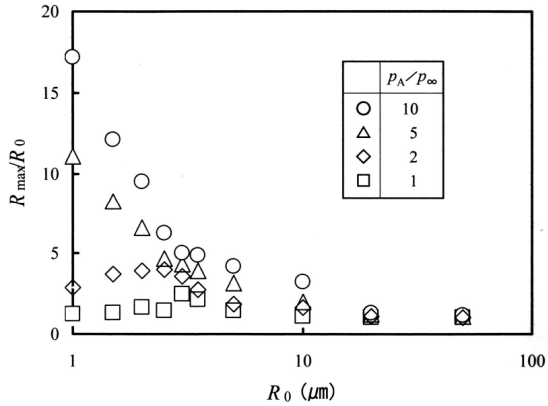

Figure 3: Maximum bubble radius versus initial bubble radius for four pressure amplitudes

Tap water and distilled water

To examine the effect of the depth H_L of a liquid on the number of cavitation bubble occurrence, tap water and distilled water were first taken as a test liquid. Figure 4 shows the cumulated number of cavitation bubbles generated in distilled water as a function of time for six values of H_L, which were obtained from the video records. The number of bubbles was counted on each frame of the video images. Obviously the maximum bubble number occurs at H_L =2.6mm. Figure 5 shows two snapshots of cavitation phenomena generated in (a) a tap water and (b) a distilled water, both of which were taken at five seconds after the ultrasound irradiation. One of the smallest bubble among three bubbles in (a), the bubble A, was measured as about 30μm in diameter. It is a natural trend that there are numerous cavitation bubbles existing in tap water in comparison with the distilled water case because tap water usually contains plenty of impurities. Figure 6 shows the maximum bubble number against the water depth, together drawing the relation between the average bubble number and the water depth. Each data point implies an averaged value obtained by employing 75 snapshots for the same experimental conditions. A solid

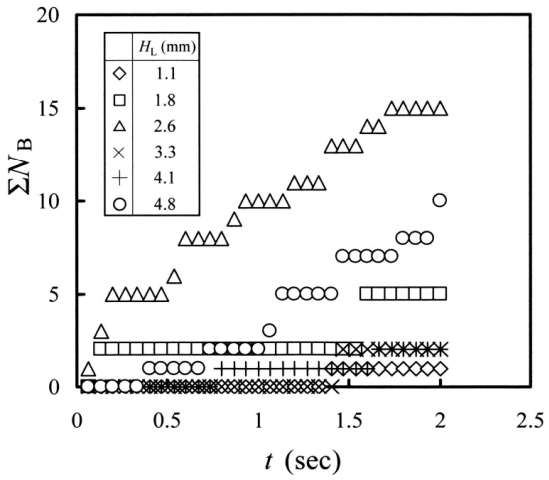

Figure 4: Cumulative number of cavitation bubbles in distilled water for six water depths (I = 1W/cm^2, x = 100%)

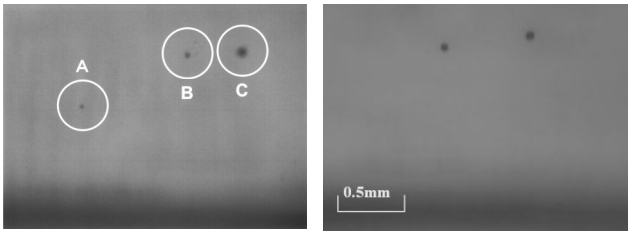

(a) (b)

Figure 5: Snapshots of cavitation bubbles generated in (a) a tap water with H_L = 2mm and (b) a distilled water with H_L = 3mm, taken at t_{ex} = 5sec after the US irradiation

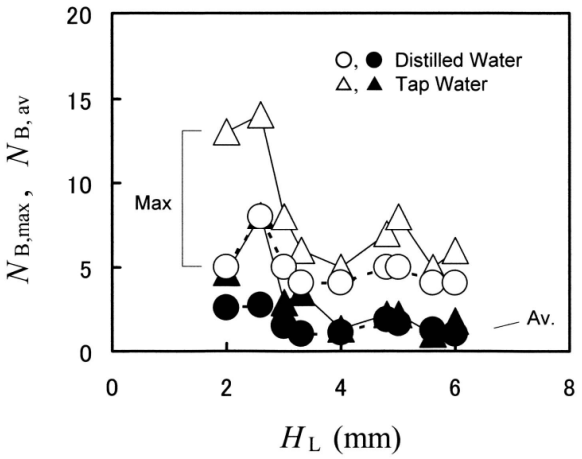

Figure 6: Maximum and average numbers of cavitation bubbles generated in a tap water and a distilled water (I =1W/cm^2, x= 100%; t_{ex} = 5sec)

symbol corresponds to the average bubble number and an open symbol expresses the maximum bubble number. Similar to Figure 4 the maximum occurs at H_L = 2.6mm (= 7λ/4). Another peak appears at 5.2mm (=14λ/4). Although the free surface may be fluctuating little by little while it is exposed to ultrasound, standing waves could be formed for these water depths, producing an enough order of negative pressure at the pressure anti-nodes where cavitation can be easily generated. Therefore, it is considered that the pressure field in the liquid is predominantly affected by the acoustically induced force, i.e. the first Bjerknes force [17]. On the contrary to this, for the shallow water case the liquid surface fluctuated violently. For some conditions a surface wave involving a number of capillary waves collapsed to disintegrate into plenty of water mass and small droplets detached from the top summit of an individual capillary wave. The impact of these matters disturbs the liquid pressure field, eventually reducing an opportunity of cavitation occurrence. Figure 7(a) shows the change of the central displacement of the free surface with time after the ultrasound irradiation for the case of H_L =1.8mm. To find out the characteristic of this wave form associated with the low frequency range a FFT analysis was conducted. The power spectrum is given in Figure 7(b). Obviously the free surface irregularly fluctuates around the average height of the free surface denoted by zero on the z axis in Figure 7(a). There are several spikes in the power spectrum, among of them two power spectra at f =2Hz and 5.2Hz are slightly prominent. It is generally known that if the amplitude of the surface fluctuation is small and the surface tension is negligibly small, the resonant frequency $f_{m,n}$ of the free surface oscillation can be expressed in the following formula[18]:

$$f_{m,n}^2 = g\xi_{m,n} \tanh (H_L\xi_{m,n} / R_V) / (4\pi^2 R_V) , \quad \text{----------} \quad (3)$$

where R_V is the radius of the cylindrical rigid vessel and H_L is the liquid depth, and m and n are integer expressing the mode of the free surface oscillation. Furthermore $\xi_{m,n}$ is the nth root of the first derivative form of the Bessel equation $J'_m(\xi) = 0$.

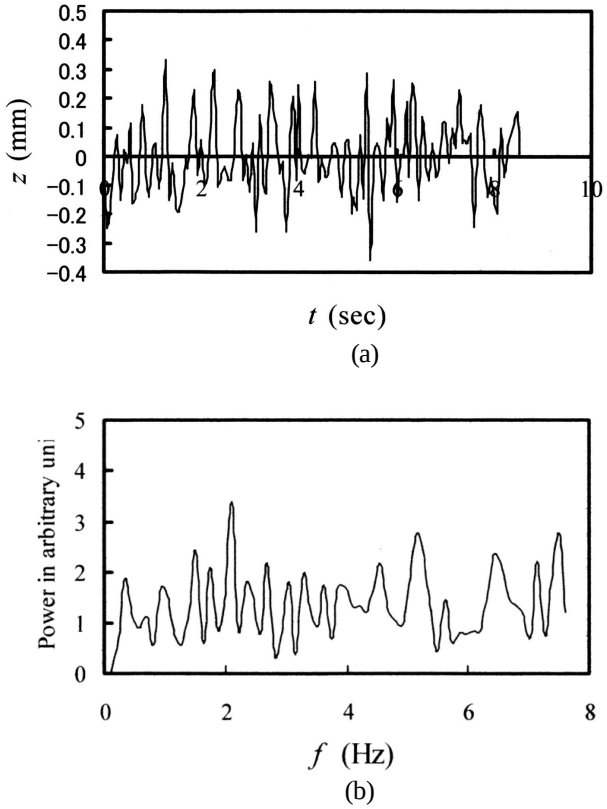

Figure 7: Free surface fluctuation of a distilled water with H_L =1.8mm where (a) variation of the vertical free surface displacement at the central part with time, (b) its power spectrum (x = 100%; H_L =1.8mm)

Equation (3) can be approximated in the form of $f = 0.293(gH)^{1/2}/R_V$ when the liquid depth H_L is small. For instance, in the case where R_V = 8mm and H_L=1.8mm, we obtain the frequency of 4.7Hz for the (1,1) mode which is close to 5.2Hz, one of the frequencies appearing in Figure 7(b). Therefore when a small amount of water is affected by the acoustic radiation pressure, the water surface fluctuates significantly, eventually breaking into pieces. Plenty of air bubbles could be entrapped into the liquid interior. This process seems to yield a different pressure field from that regarding the deep water case.

Microbubble suspension

Sonazoid microbubble suspension is in non-transparency before US irradiation, looking milky-white color due to light scattering from minute bubbles uniformly dispersed in distilled water. However once Sonazoid suspension is exposed to ultrasound waves, it becomes to be transparent within a very short time that means that microbubbles are destroying. Figure 8 shows one example of images taken from the digital video photography at the time of 66ms after the US irradiation for the H_L =2.6mm case. The ultrasound waves were radiated from the below, propagating through the vessel bottom and passing through into the interior of the suspension. As clearly seen the transparency is high. This feature results from the acoustic cracking of microbubbles because C_4F_{10} gas was flowed out when the 4nm thick shell of an individual microbubble was crushed. The microbubble disruption

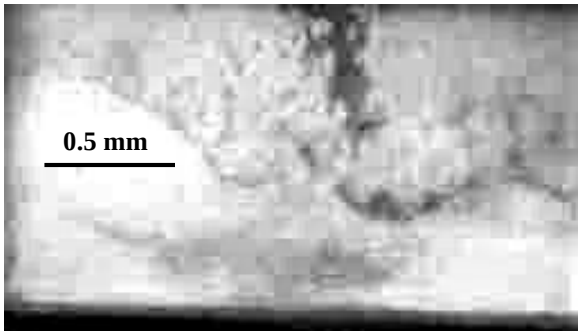

Figure 8: Sonic cracking of microbubbles observed at 66ms after the US irradiation (x = 100%; H_L = 2.6mm)

propagates upward, and the resultant debris also flows upward. Then it floats and circulates almost synchronized with the acoustic streaming. The second product consisting of the C_4F_{10} gas and crushed shells can remain for a relatively long time and it can play an important role as cavitation nuclei, affecting the pressure and velocity fields. Figure 9 shows the microbubble destruction as a function of the exposure time for various liquid depths, indicating the relationship between the microbubble survival number N_{MB}/N_{MB0} with N_{MB0} being an initial average number of Sonazoid microbubbles and the ultrasound exposure time t_{ex}. In this figure open symbols correspond to the case where the intensity I is 1W/cm^2 and the repetition number N_P of 2000 pulses, a large solid triangle (▲) is the case where I = 1W/cm^2, N_P = 500pulses and H_L=3.0mm, and a small open triangle (△) is the case where I = 0.24W/cm^2, N_P = 2000pulses and H_L = 3.0mm. Before the US irradiation the N_{MB0} was measured as forty-four on average. Microbubbles are destroyed quickly, reducing the survival number to half of N_{MB0} when the exposure time is about 100ms. At the exposure time of one second only a few number of microbubbles were able to count under a microscope. However it should be noted that an extremely numerous microbubbles still remained within the suspension. For instance, if there is one microbubble existing in the microscopic measuring area, more than 40,000 microbubbles are still alive within the observation domain V_0 of 14mm^3. Furthermore a special feature was found that the survival number versus exposure curve is less dependent on the liquid depth. This suggests that the microbubble destruction is dominantly attributed to the acoustic radiation pressure which must be a cause of a sonic cracking. It is seen that the survival number for N_P = 500pulses is slightly larger than the N_P = 2000pulses case except for the time around 400ms. On the other hand the microbubble disruption is strongly affected by the intensity of ultrasound. In fact when it was 0.24W/cm^2, denoting with a small open triangle, only 40% microbubbles were destroyed up to one second, while more than 90% microbubbles were crushed for the 1W/cm^2 case. To observe the microbubble destruction and cavitation bubble behavior, a great deal of snapshots have been taken. Figure 10 shows two snapshots taken for the repetition of 500 pulses with the duty ratio of x = 50% and Figure 11 for 2000 pulses with x = 50%, both of which obtained for the liquid depth of 3mm. The light flash duration of these pictures was 2μs. Darkness was covered until 250ms for the case where N_p = 500 pulses. The transparency started from near the

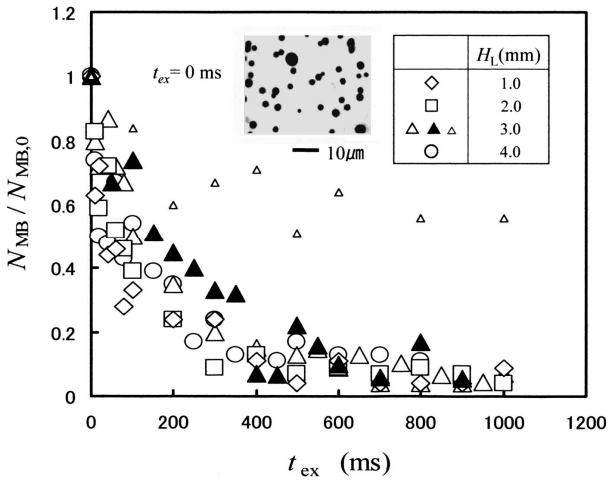

Figure 9: Survival number of microbubbles versus exposure time for four liquid depths, where open symbols correspond to the data for I = 1.0W/cm^2, x = 50% and N_p = 2000 pulses; ▲: I = 1.0 W/cm^2, x = 50% and N_p = 500 pulses; △ : I = 0.24W/cm^2, x = 50% and N_p = 2000 pulses

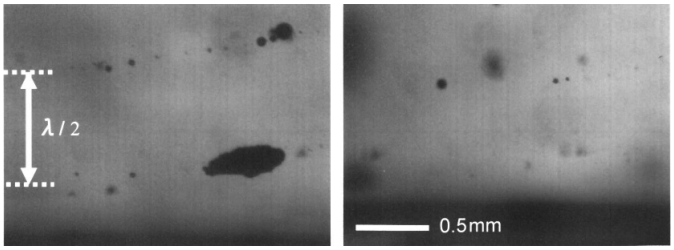

(a) (b)

Figure 10: Interaction of ultrasound waves with microbubbles and induced cavitation bubbles: (a) 450ms, (b) 900ms (I = 1 W/cm^2, x = 50%, N_p=500 pulses; H_L = 3mm)

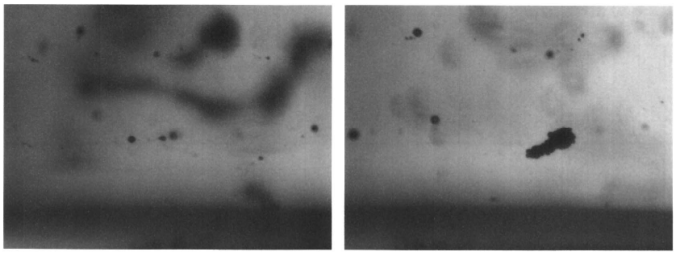

(a) (b)

Figure 11: Interaction of ultrasound with microbubbles and induced cavitation bubbles: (a) 650ms, (b) 950ms (I = 1W/cm^2, x = 50%, N_p = 2000 pulses; H_L = 3mm)

vessel bottom due to sonic cracking. In Figure 10(a) cavitation bubbles are visible at the upper part, where the pressure anti-node was formed. There is another line of cavitation bubbles including a debris at a definite interval from the upper line, that is almost a half of the wave length of the 1MHz ultrasound wave. The debris must be consisting of numerous crushed shells of microbubbles, which can gather due to cohesion. The number of cavitation bubbles decreases as increasing the exposure time as obviously seen in Figures 10(b) and 11(b). Cavitation phenomena tend to

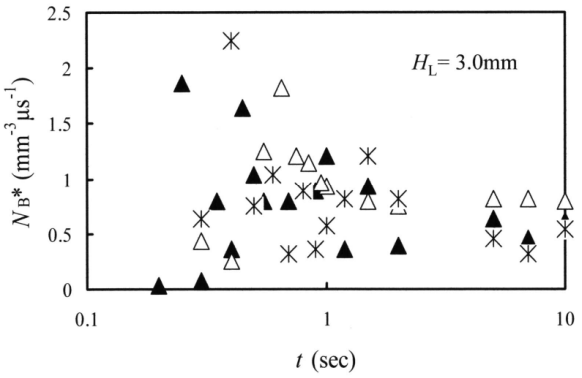

Figure 12: Time dependency of the number of cavitation bubbles per unit volume and per unit exposure time N_B* mm^{-3}μs^{-1} for H_L = 3mm (∗: x=100%, ▲: x=50%; 500pulses, Δ: x=50%; 2000 pulses)

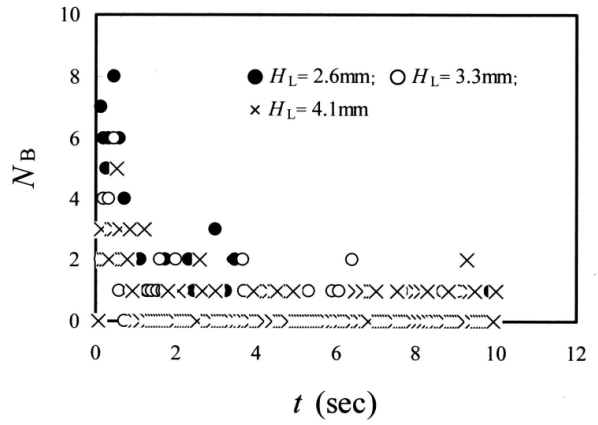

Figure 13: Variation of the number of cavitation bubbles with time for three different depths, where the data were obtained from the long-term video images (I = 1W/cm^2, x = 100 %)

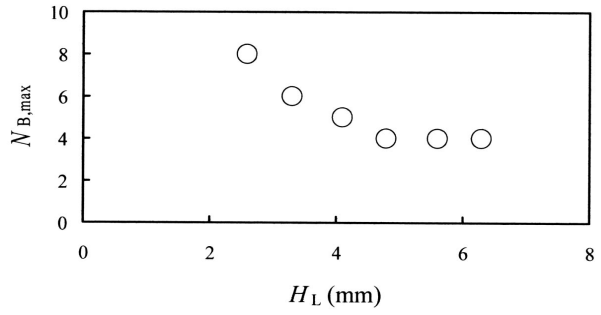

Figure 14: Maximum number of cavitation bubbles $N_{B,max}$ versus liquid depth H_L (I = 1W/cm^2, x =100%)

occur in the neighborhood of the second products of microbubbles. Time dependency of the number of cavitation bubbles per unit volume and per unit time N_B* (= N_B / (V_0 t_d)) is summarized in Figure 12 for the case of H_L =3mm. These data were all obtained from the snapshots. In the figure an asterisk denotes the data for continuous waves with the duty ratio of x=100%, an open triangle and a solid triangle imply the data for x = 50% with N_p = 2000pulses and for x = 50% with N_p =500pulses,

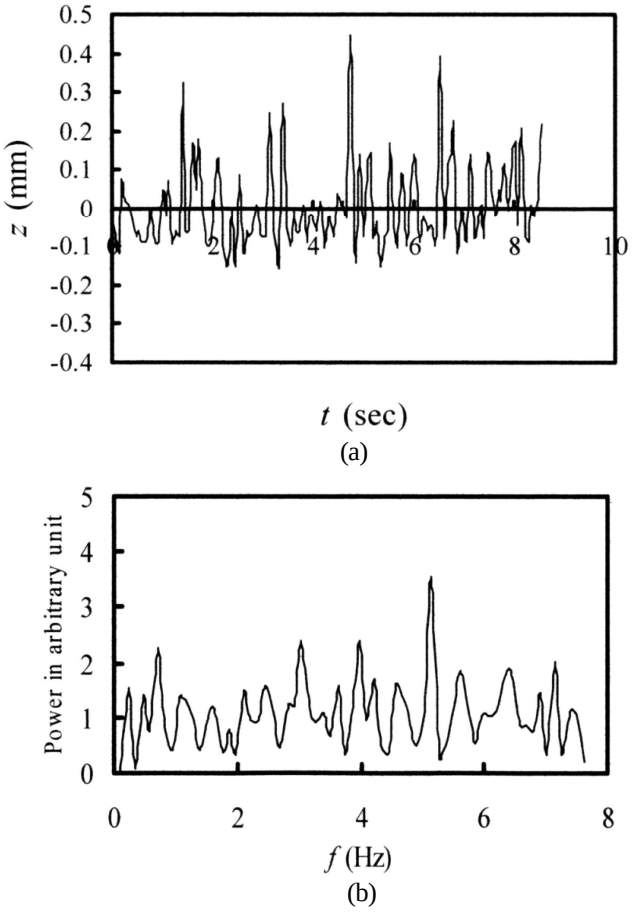

Figure 15: Free surface fluctuation of a 10 % v/v Sonazoid microbubble solution with the conditions of H_L = 1.8mm and x = 100%: (a) variation of the vertical displacement of the free surface at the central part with time; (b) its power spectrum

respectively. It is found that N_B* is attained to a maximum number at a certain exposure time less than one second where more than sixty cavitation bubbles were generated. Obviously no difference is found in the number of cavitation bubbles, N_B*, between the two cases, i.e. the data obtained from the burst pressure waves and those obtained from the continuous waves. Figure13 shows the comparison of the number of cavitation bubbles as a function of time for three different depths of Sonazoid suspension (x=100%), which were obtained from the long-term video images. It should be mentioned that the number of cavitation bubbles in Figure 13 was apt to be less counted by about one seventh of the data obtained from the snapshots. A main reason comes from a difference in lighting, but details are still unknown. Again the bubble number reaches the maximum sometime before one second after the US irradiation, afterward it slightly fluctuates around a certain value. In Figure 14 the maximum cavitation bubble number $N_{B,max}$ is examined for the liquid depth H_L. It is clear that $N_{B,max}$ increases as decreasing H_L, while it approaches to a constant value in the range of H_L > 4.8mm. Similar to Figure 7, when the liquid depth is shallow the free surface is strongly affected by the ultrasound radiation pressure. Consequently a significant fluctuation occurs at the free surface, inducing various kinds of the modes of the surface oscillation. For a Sonazoid suspension the free surface oscillation was observed with the high-speed video

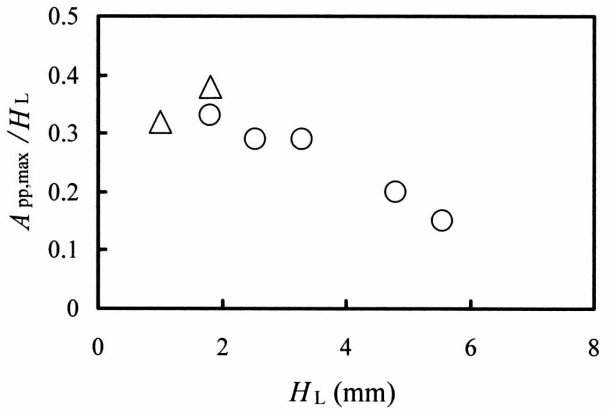

Figure 16: Dimensionless maximum amplitude $A_{pp,max}$ of a free surface with the definition of peak to peak amplitude which is divided by the liquid depth H_L (I = 1W/cm^2, x = 100%)

photography for the same liquid depth of H_L= 1.8mm as the distilled water case. Figure 15 is the result indicating (a) the free surface displacement and (b) its power spectrum. There are several spikes in the power spectrum. In particular a prominent power appears at the frequency of about 5Hz, which is close to the resonant frequency of the (1,1) mode. Of cause the actual surface fluctuation must be complicated and contained a wide range of frequencies including the higher orders of components as well as involving a large number of capillary spikes. To find out the resonant frequencies with higher orders a more accurate measurement should be made by taking photographs with a sufficient time resolution. Nevertheless the occurrence of the (1,1) mode suggests that the free surface of Sonazoid suspension must be linearly declined with time and one of the outer-edge of the surface alternately moves downward and upward with the frequency of about 5Hz. This seems important because the flow induced by this surface oscillation must be relevant to the evidence of second products to be conveyed everywhere in the liquid. As a result cavitation bubbles can be created at a relatively longer time after the ultrasound irradiation even though the majority of microbubbles are destroyed during an earlier period. Figure 16 shows the dimensionless maximum amplitude of the free surface at the central part, defined as the peak to peak amplitude $A_{pp,\,max}$ which is divided by the liquid depth H_L. The maximum value of $A_{pp,\,max}/H_L$ occurs at around H_L= 2.0mm where the largest fluctuation is achieved. For the shallow liquid case, therefore, a complex flow may be caused in the liquid, preventing the formation of standing waves. As mentioned above, only a few cavitation bubbles were created at a later time over one second. However, occasionally numerous number of cavitation bubbles were generated at a later exposure time, e.g. five to ten seconds which are frequently employed *in vitro* experiment. A typical example is shown in Figure 17 for the case where H_L = 4mm and t_{ex} = 5 sec. The exposure time of five seconds is enough for mixing the liquid as a whole due to the mixing effect of the acoustic radiation and the liquid surface fluctuation. It is, therefore, conjectured that the probability of cavitation nuclei to be carried to the area near the vessel bottom, where cells are usually attached to, must be elevated in *in vitro* experiment.

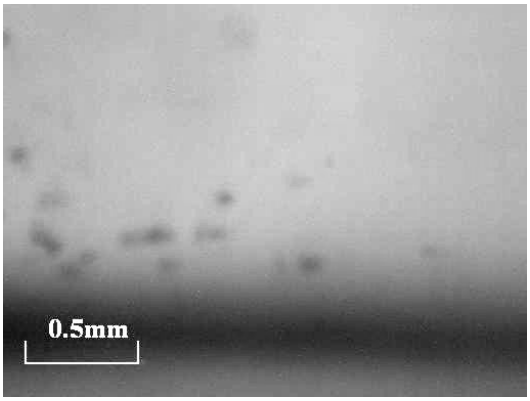

Figure 17: A snapshot taken at 5sec after the US irradiation, indicating a number of cavitation bubbles generated in a Sonazoid microbubble suspension near the bottom of the vessel (x = 100%; H_L = 4mm)

CONCLUSIONS

The results obtained here can be summarized in the following.

(1) In the cases of both tap water and distilled water, the maximum number of cavitation bubbles occurred at the water depth of 2.6mm. Under this condition standing waves were formed. Cavitation bubbles are apt to generate at near the pressure anti-nodes. As decreasing the water depth the number of cavitation bubbles decreased.

(2) When a Sonazoid suspension was irradiated by the ultrasound waves microbubbles were destroyed quickly, decreasing to half the number of original Sonazoid micro-bubbles at the exposure time of about 100ms.

(3) The destruction of microbubbles is significantly affected by the sound intensity, but less influenced by the liquid depth. It is found that microbubble destruction is slightly stronger in the case of N_p=2000 pulses in comparison with the N_P=500 pulses case.

(4) A large number of cavitation bubbles were generated within one second after the ultrasound irradiation in a Sonazoid suspension.

(5) In a Sonazoid microbubble suspension, the second products consisting of C_4F_{10} gas and the debris of the crushed shell seem to remain for a relatively longer period due to the flow induced by the surface oscillation as well as by the acoustic radiation pressure. Therefore cavitation can occur even at a later period after the ultrasound irradiation, and sometimes reveals in the form of a large number of bubbles.

ACKNOWLEDGMENTS

The authors would like to express their thanks to Mr. Y. Hamada of SANPICO Ltd. for his assistance in high-speed photography. YT was supported by a grant from the Japan Society for the Promotion of Science for the Grant-in Aid for Scientific Research (C) (20560144). TK acknowledges the Grant-in Aid for Scientific Research (B) (20300173); the Grant-in-Aid for Exploratory Research (21650124); the Grants-in-Aid for Scientific Research on Priority Area, MEXT (20015005);

and the Grant for Research on Advanced Medical Technology, the Ministry of Health, Labour and Welfare of Japan (H19-nano -010). A financial support was received from the Knowledge Creation Technology Co., Ltd. with many thanks.

APPENDIX

The motion of a cavitation bubble can be expressed by applying a Keller-Miksis model with the accuracy of the first order liquid compressibility as follows[16]:

$$R\ddot{R}\left(1-\frac{\dot{R}}{c}\right)+\frac{3}{2}\dot{R}^2\left(1-\frac{\dot{R}}{3c}\right) = \left(1+\frac{\dot{R}}{c}\right)\frac{1}{\rho}\left[p_{r=R}(R,t)-p_c\left(t+\frac{R}{c}\right)-p_\infty\right]+\frac{R}{\rho c}\bullet\frac{dp_{r=R}(R,t)}{dt}, \quad \text{---------- (A1)}$$

where R is the bubble radius, t the time, ρ the liquid density, μ the liquid viscosity, σ the surface tension, c the sound velocity in liquid and p_∞ the pressure in liquid at infinity. The bubble wall pressure $p_{r=R}$ is written as

$$p_{r=R}(R,t)=\left(p_\infty+\frac{2\sigma}{R_0}\right)\left(\frac{R_0}{R}\right)^{3\gamma}-\frac{2\sigma}{R}-\frac{4\mu}{R}\dot{R} \quad \text{---------- (A2)}$$

In addition the oscillatory pressure term $p_c(t)$ is given as

$$p_c(t)=p_A\sin\omega t=p_A\sin(2\pi ft), \quad \text{---------- (A3)}$$

where p_A is the pressure amplitude and ω the angular frequency.

NOMENCLATURE

c	sound velocity	[m/s]
E	ultrasound energy density	[J/m^2]
f	frequency	[1/s]
H_L	liquid depth	[m]
I	sound intensity	[W/cm^2]
L_s	distance from vibrating surface to free surface	[m]
N_B	number of cavitation bubbles	[-]
N_{MB}	number of microbubbles	[-]
N_p	pulse number of ultrasonic waves	[-]
t_{ex}	exposure time	[s]
x	duty ratio	[%]
λ	wave length (= c/f)	[m]

REFERENCES

[1] Kodama, T., Tomita, Y., Koshiyama, K. and Blomley, M.J.K. 2006, "Transfection effect of microbubbles on cells in superposed ultrasound waves and behavior of cavitation bubble," *Ultrasound in Med.& Biol.*, 32-6, 905-914.

[2] Kodama, T., Tomita, Y., Watanabe, Y., Koshiyama, K.,Yano, T. and Fujikawa, S. 2009, "Cavitation bubbles mediated molecular delivery during sonoporation, " *Journal of Biomechanical Science and Engineering, JSME*, Vol.4, No.1, 124-140 (2009).

[3] Postema, M., van Wamel, A., Lancee, C. and de Jong, N. 2004,"Ultrasound-induced encapsulated microbubble phenomena," *Ultrasound in Med. & Biol.*, 30-6, 827-840.

[4] Kodama, T. and Tomita, Y. 2000, "Cavitation bubble behavior and bubble-shock wave interaction near a gelatin surface as a study of in vivo bubble dynamics", Applied Physics B: Lasers and Optics, 70-1, 139-149.

[5] Brujan, E. A. 2004,"The role of cavitation microjets in the therapeutic applications of ultrasound", *Ultrasound in Med.& Biol.*, 30-3, 381-387.

[6] Bao, S., et al. 1997, "Transfection of a reporter plasmid into cultured cells by sonoporation *in vitro*", *Ultrasound in Med.& Biol.*, 23-6, 953-959.

[7] Tomita, Y. and Shima, A. 1986, "Mechanisms of impulsive pressure generation and damage pit formation by bubble collapse, "*Journal of Fluid Mechanics*, 169, 535-564.

[8] Philipp, A. and Lauterborn, W. 1998, "Cavitation erosion by single laser-produced bubbles", *Journal of Fluid Mechanics*, 361, 75-116.

[9] Kodama, T., Hamblin, M.R. and Doukas, A.G. 2000, "Cytoplasmic molecular delivery with shock waves: importance of impulse", *Biophysical Journal*, 79-4, 1821-1832.

[10] Doukas, A.G., McAuliffe, D.J. and Flotte, T.J. 1993, " Biological effects of laser-induced shock waves: structural and functional cell damage *in vitro*", *Ultrasound in Med.& Biol.*, 19-2, 137-146.

[11] Ohl, C.D. and Ikink, R.,"Shock-wave-induced jetting of micron size bubbles", *Phys. Rev. Lett.*, 90-21, 214502-214505.

[12] Koshiyama, K., Kodama,T., Yano,T. and Fujikawa, S. 2006," Structual change in liquid bilayers and water penetration induced by shock waves: molecular dynamics simulations", *Biophysical Journal*, 91-6, 2198-2205.

[13] Prentice, P., Cuschieri, A., Dholakia, K., Prausnitz, M. and Campbell, P. 2005," Membrane disruption by optically controlled microbubble cavitation", Nature Physics, 1, 107-110.

[14] Hoff, L. 2001, "Acoustic Characterization of Contrast Agents for Medical Ultrasound Imaging," *Kluwer Academic Publishers*.

[15] http://www.tuat.ac.jp/~yamada/onkyo/chap4/chap4.html

[16] Keller, J.B. and Miksis, M. 1980, "Bubble oscillations of large amplitude", *Journal of the Acoustical Society of America*, 68-2, 628-633.

[17] Crum, Lawrence A. 1975, "Bjerknes forces on bubbles in a stationary sound field", *Journal of the Acoustical Society of America*, 57-6, 1363-1370.

[18] Moiseev, N.N. and Petrov, A.A. 1966, "The calculation of free oscillations of a liquid in a motionless container", In Advances in Applied Mechanics, Vol.9 (edited by Richard von Mises), *Academic Press.*